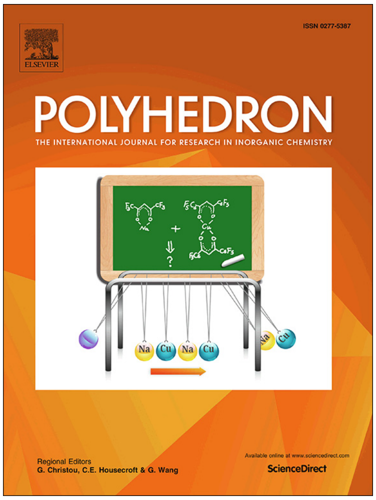

Reactivity and structural patterns of phenylphosphines in acetylene and acetylide carbonyl trinuclear ruthenium clusters

Erik G. Rojo–Gómez, Abril I. Munguía–Lara, Daniel O. González–Abrego, Gloria Sánchez–Cabrera, José G. Alvarado–Rodríguez, María G. Hernández –Cruz, María J. Rosales–Hoz, Marco A. Leyva, Ana L. Carrasco, Noemí Andrade–López, Francisco J. Zuno–Cruz

PII: S0277-5387(19)30035-X
DOI: https://doi.org/10.1016/j.poly.2019.01.020
Reference: POLY 13693

To appear in: *Polyhedron*

Received Date: 28 September 2018
Revised Date: 12 December 2018
Accepted Date: 9 January 2019

Please cite this article as: E.G. Rojo–Gómez, A.I. Munguía–Lara, D.O. González–Abrego, G. Sánchez–Cabrera, J.G. Alvarado–Rodríguez, M.G. Hernández–Cruz, M.J. Rosales–Hoz, M.A. Leyva, A.L. Carrasco, N. Andrade–López, F.J. Zuno–Cruz, Reactivity and structural patterns of phenylphosphines in acetylene and acetylide carbonyl trinuclear ruthenium clusters, *Polyhedron* (2019), doi: https://doi.org/10.1016/j.poly.2019.01.020

Reactivity and structural patterns of phenylphosphines in acetylene and acetylide carbonyl trinuclear ruthenium clusters

Erik G. Rojo–Gómez[a,1], Abril I. Munguía–Lara[a,1], Daniel O. González–Abrego[a], Gloria Sánchez–Cabrera[a*], José G. Alvarado–Rodríguez[a], María G. Hernández−Cruz[b], María J. Rosales–Hoz[c], Marco A. Leyva[c], Ana L. Carrasco[c], Noemí Andrade–López[a], Francisco J. Zuno–Cruz[a,*]

[a] *Centro de Investigaciones Químicas, Universidad Autónoma del Estado de Hidalgo, Ciudad Universitaria, Carretera Pachuca−Tulancingo km 4.5. Colonia Carboneras, Mineral de la Reforma, Hidalgo. 42184, México*

[b] *Universidad Juárez Autónoma de Tabasco, División Académica Multidisciplinaria de Jalpa de Méndez, Carr. Estatal Libre VHS−COM. km. 27+000 s/n Rancho, Ribera Alta, Jalpa de Méndez, Tabasco 86205, México*

[c] *Departamento de Química, Centro de Investigación y de Estudios Avanzados, Av. Instituto Politécnico Nacional 2508, Col. San Pedro Zacatenco, Ciudad de México 07360, México*

Abstract

The acetylene $[Ru_3(\mu\text{–}CO)(CO)_9\{\mu_3\text{–}\eta^2\text{–}(//)\text{–}HC{\equiv}C\text{–}R\}]$ (**1a**: R = $C(Me){=}CH_2$); **1b**: R = $\overline{C{=}CH\text{–}(CH_2)_3\text{–}CH_2}$) and the acetylide $[Ru_3(\mu\text{–}H)(CO)_9\{\mu_3\text{–}\eta^2\text{–}(\perp)\text{–}C{\equiv}C\text{–}R\}]$ (**2a**: R = $C(Me){=}CH_2$; **2b**: R= $\overline{C{=}CH\text{–}(CH_2)_3\text{–}CH_2}$) clusters have been synthesized from the reaction

---

[1] Both authors contributed equally to the work presented in this paper.

[*] Corresponding Authors. Phone: work +52─771─7172000 ext 2204; cell +52─1771─1625212; Fax: +52─771─7172000 ext 6502.

E─mail address: fjzuno@uaeh.edu.mx (F. J. Zuno─Cruz).

of $[Ru_3(CO)_{10}(NCMe)_2]$ with 2–methyl–1–buten–3–yne and 1–ethynylcyclohexene respectively. The reactions of the corresponding parallel acetylene **1a** or **1b** with triphenylphosphine or diphenylmethylphosphine yielded four isostructural compounds $[Ru_3(\mu\text{–}CO)(CO)_8(L)\{\mu_3\text{–}\eta^2\text{–}(//)\text{–}HC{\equiv}C\text{–}R\}]$ (**3a1**: L = PPh_3, **3a2**: L = PPh_2Me, R = $C(Me){=}CH_2$; **3b1**: L = PPh_3, **3b2**: L = PPh_2Me, R = $\overline{\mathrm{C{=}CH{-}(CH_2)_3{-}CH_2}}$) where, the alkynes are still coordinated to the metallic fragment as acetylene groups in a $\mu_3\text{–}\eta^2$ parallel fashion. Also, the isomer compounds $[Ru_3(\mu\text{–}H)(CO)_8(L)\{\mu_3\text{–}\eta^2\text{–}(\perp)\text{–}C{\equiv}C\text{–}R\}]$ (**4a1** and **5a1**: L = PPh_3, **4a2** and **5a2**: L = PPh_2Me, R = $C(Me){=}CH_2$; **4b1** and **5b1**: L = PPh_3, **4b2** and **5b2**: L = PPh_2Me, R = $\overline{\mathrm{C{=}CH{-}(CH_2)_3{-}CH_2}}$); and the disubstituted phenylphosphine clusters $[Ru_3(\mu\text{–}H)(CO)_7(L)_2\{\mu_3\text{–}\eta^2\text{–}(\perp)\text{–}C{\equiv}C\text{–}R\}]$ (**6a1**: L = PPh_3, **6a2**: L = PPh_2Me, R = $C(Me){=}CH_2$; **6b1**: L = PPh_3, **6b2**: L = PPh_2Me, R = $\overline{\mathrm{C{=}CH{-}(CH_2)_3{-}CH_2}}$) were formed during each reaction. In these compounds, the parallel–acetylene group undergoes an oxidative addition and a rearrangement of the coordinated organic fragment to a $\mu_3\text{–}\eta^2$ perpendicular coordination mode of the C–C axis by breaking acetylene C–H bond to give a hydride ligand in each case. The synthesis of clusters $[Ru_3(\mu\text{–}CO)(CO)_8(PPh_3)\{\mu_3\text{–}\eta^2\text{–}(//)\text{–}HC{\equiv}C\text{–}C_6H_2\text{–}2,4,5\text{–}Me_3\}]$ (**3c1**), $[Ru_3((\mu\text{–}H)(CO)_8(PPh_3)\{\mu_3\text{–}\eta^2\text{–}(\perp)\text{–}C{\equiv}C\text{–}C_6H_2\text{–}2,4,5\text{–}Me_3\}]$ (**4c1** and **5c1**) and $[Ru_3(\mu\text{–}H)(CO)_7(PPh_3)_2\{\mu_3\text{–}\eta^2\text{–}(\perp)\text{–}C{\equiv}C\text{–}C_6H_2\text{–}2,4,5\text{–}Me_3\}]$ (**6c1**) are also described. All compounds have been characterized in solution by infrared spectroscopy and by ^1H, $^{13}C\{^1H\}$ and $^{31}P\{^1H\}$ NMR. The molecular structures of compounds **2b**, **3a1**, **3b1**, **4a1**, **4c1**, and **6b1** have been established by single crystal X–ray diffraction studies.

Keywords: Ruthenium; Clusters; Acetylenes; Acetylides, Phenylphosphines

1. Introduction

Carbonyl trinuclear ruthenium clusters still attract the long−standing interest on their synthetic and reactivity features. [1-4] This interest is mainly due to the ease and straight forward synthetic methods to yield them, helping to establish their chemical behavior, structural patterns, and spectroscopic characteristics, obtained when they react with either organic or inorganic ligands [5,6]. It is well known that the reaction of $[Ru_3(CO)_{12}]$ with terminal alkynes has been the source of μ_3–η^2 parallel coordination mode of the –C≡C–H moiety in triruthenium clusters; these clusters subsequently undergo a facile H−migration from carbon to the cluster, involving a coordination rearrangement to give the μ_3–η^2 acetylide–hydrido perpendicular complexes [7,8]. In addition, alkynes and phosphine ligands are representative substrates to explore the multiple two−electron donor ligand capabilities in cluster chemistry [5,9-11], where phosphine or phosphite ligands have been considered as binder agents that provide stability to the metal core with potential implications in catalytic hydrogenation reactions [12-16]. Despite the great amount of reactions between carbonyl clusters and phosphines, the reactivity of cluster complexes with coordinated alkynes have been less explored.

The aim of the present work is the synthesis and structural characterization of three new series of μ_3–η^2 parallel–acetylene and perpendicular–acetylide triruthenium clusters, obtained from ene–yne and alkyne ligands and used in phosphine substitution reactions. All compounds were characterized in solution by Infrared and by ^1H, $^{13}C\{^1H\}$ and $^{31}P\{^1H\}$ NMR spectroscopies and by 2D–heteronuclear correlation experiments for the complete assignment of carbon atoms. The assignment of phosphorous atoms in compounds were determined using heteronuclear irradiation experiments. The molecular structures of compounds **2b**, **3a1**, **3b1, 4a1**, **4c1**, and **6b1** in the solid state were determined by single crystal X–ray diffraction studies.

2. Experimental Section

2.1 General procedures and materials

$[Ru_3(CO)_{10}(NCMe_3)_2]$, $[Ru_3(\mu–CO)(CO)_9\{\mu_3–\eta^2–(//)–HC\equiv C–C_6H_2–2,4,5–Me_3\}]$ (**1c**) and $[Ru_3(\mu–H)(CO)_9\{\mu_3–\eta^2–(\perp)–C\equiv C–C_6H_2–2,4,5–Me_3\}]$ (**2c**) were prepared by published methods [8]. Trimethylamine *N*–oxide was dried and purified prior to use. All other chemicals were purchased from Aldrich Company and used as received. All reactions were performed under a nitrogen atmosphere by using standard Schlenk techniques. Solvents were dried by the standard procedures prior to use. Commercial TLC plates (silica gel 60 F254) were used to monitor the progress of the reactions. Infrared spectra were recorded as either solid thin films in a CsI window on a GX PERKIN Elmer 2000 FT–IR spectrophotometer or in NaCl cells on a PERKIN Elmer 16FPCFPIR spectrophotometer. Mass spectrometric measurements were performed by direct insertion on a HR–LC 1100/MSD TOF Agilent Technology equipment at CINVESTAV–México. NMR spectra were measured on a VARIAN 400 and a Bruker 400 spectrometers in $CDCl_3$, with ^1H and ^{13}C spectra relative to $SiMe_4$, and ^{31}P spectra relative to 85% aq. H_3PO_4. Full assignment of ^1H, $^{13}C\{^1H\}$ and $^{31}P\{^1H\}$ NMR for all synthesized compounds can be found in supporting information (SI) file.

2.2 Single crystal X-Ray studies

Suitable crystals of **2b** and **4a1** were selected and collected on an Enraf–Nonius Kappa CCD area detector diffractometer with graphite–monochromated Mo–$K\alpha$ radiation. Data were integrated, scaled, sorted, and averaged using the package, HKL Scalepack by Otwinowsky [17], the structure was solved with the SHELXS/2016 [18] structure solution program using Direct Methods and refined with the SHELXL 2016/6 [19] refinement package using Least Squares minimization. Data for **3b1** were collected on a Bruker D8 Venture diffractometer using Mo–$K\alpha$ radiation. Data collection, determination of unit cell, and integration of frames of this compound were carried out using the Bruker APEX3 software [20,21]. A semi–empirical absorption correction method (SADABS) [22] was applied. The structure was solved by Direct Methods, completed by subsequent difference Fourier synthesis, and refined by full–matrix least–squares on F^2 procedures using the SHELX–2014–7 package [18]. Crystallographic programs were used under WINGX suite [23]. Suitable crystals of **3a1**, **4c1**, **6b1**, and **6c1** were selected and collected on a Xcalibur, Atlas, Gemini diffractometer. The crystals were kept at 294 K during data collection. Using Olex2 [24], the structure were solved with the ShelXT [25] structure solution program using Intrinsic Phasing and refined with the ShelXL [19] refinement package using Least Squares minimization. For all compounds, all non–hydrogen atoms were refined anisotropically. The positions of the hydrogen atoms were kept fixed with a common isotropic displacement parameter. Crystallographic and other experimental data are summarized in Table 1.

Table 1. Crystal data and structure refinement parameters of compounds **2b**, **3a1**, **3b1**, **4a1**, **4c1** and **6b1**.

Compound	**2b**	**3a1**	**3b1**	**4a1**	**4c1**	**6b1·2CHCl₃**
Empirical formula	$C_{17}H_{10}O_9Ru_3$	$C_{32}H_{21}O_9P_1Ru_3$	$C_{35}H_{25}O_9P_1Ru_3$	$C_{31}H_{21}O_8P_1Ru_3$	$C_{37}H_{27}O_8P_1Ru_3$	$C_{53}H_{42}O_7P_2Cl_6Ru_3$
Formula weight	661.46	883.67	923.75	855.66	933.76	1368.71
Crystal color	Yellow	Yellow	Yellow	Yellow	Yellow	Orange
Crystal system	Triclinic	Monoclinic	Triclinic	Triclinic	Monoclinic	Triclinic
Crystal size (mm^3)	0.28×0.15×0.12	0.20×0.20×0.10	0.31×0.21×0.15	0.15×0.08×0.03	0.30×0.2×0.2	0.60×0.50×0.50
Space group	$P-1$	Cc	$P-1$	$P-1$	$P2_1/n$	$P-1$
a (Å)	9.1531(2)	15.6889(8)	9.0880(3)	9.5113(3)	9.3377(3)	12.3117(2)
b (Å)	9.3234(2)	9.8603(4)	10.9049(3)	10.5678(3)	32.2765(10)	16.2801(3)
c (Å)	14.5625(3)	23.3770(14)	18.7091(5)	16.3762(5)	12.6005(5)	16.6746(3)
α (°)	76.6930(10)	90.00	75.778(10)	81.7000(10)	90.00	117.7915(18)
β (°)	81.0110(10)	113.964(7)	77.828(10)	77.7190(10)	109.530(4)	90.2235(13)
γ (°)	63.1370(10)	90.00	81.345(0)	84.0590(10)	90.00	103.5485(15)
V, (Å^3)	1076.91(4)	3304.6(3)	1747.36(9)	1587.00(8)	3579.2(2)	2849.42(10)
Z	2	4	2	2	4	2
$D_{calcd,}$ (Mg m^{-3})	2.040	1.776	1.7556	1.791	1.733	1.595
μ, (mm^{-1})	2.120	1.453	1.378	1.507	1.345	1.170
2θ range (°)	7.40 to 54.90	5.76 to 52.108	5.82 to 54.96	7.70 to 53.82	5.98 to 52.74	6.006 to 52.744
Index ranges	−11/11, −11/12, −18/18	−19/19, −12/12, −28/28	−11/11, −14/12, −24/24	−11/11, −11/13, −16/20	−11/11, −40/40, −15/15	−15/15, −20/20, −20/20
Reflections collected	21059	17045	27902	21179	46279	117670
Independent reflections	4884 (R_{int} = 0.0310)	6474 (R_{int} = 0.0505)	8027 (R_{int} = 0.0303)	6628 (R_{int} = 0.0500)	7318 (R_{int} = 0.0514)	11640 (R_{int} = 0.0339)
Observed reflections	4036 [I>2σ(I)]	5663 [I>2σ(I)]	6973 [I>2σ(I)]	4895 [I>2σ(I)]	5839 [I>2σ(I)]	9653 [I>2σ(I)]
Parameters/restraints	322/106	407/2	441/0	393/0	449/0	586/72
R final; R all data	0.0293, 0.0405	0.0523, 0.0625	0.0420, 0.0491	0.0402, 0.0696	0.0318, 0.0507	0.0545, 0.0702
R*w* final, R*w* all data	0.0755, 0.0707 [a]	0.1245, 0.1314 [b]	0.1071, 0.1114 [c]	0.0727, 0.0820 [a]	0.0512, 0.0577 [d]	0.1414, 0.1594 [e]
GOF (all data)	1.040	1.116	1.091	1.077	1.100	1.077
Max, min peaks (eÅ^{-3})	0.782 /−0.533	1.490 /−0.670	2.216 /−1.339	0.653 /−0.787	0.655 /−0.374	2.505 /−1.138

[a] $w^{-1} = \sigma^2(F_o^2)+(P)^2 + P$. [b] $w^{-1} = \sigma^2(F_o^2)+(0.0689P)^2$. [c] $w^{-1} = \sigma^2(F_o^2)+(0.0356P)^2 + 5.2357P$. [d] $w^{-1} = \sigma^2(F_o^2)+(0.\ 0143P)^2 + 2.4260P$. [e] $w^{-1} = \sigma^2(F_o^2)+(0.0729P)^2 + 10.5499P$. Where $P = (F_o^2+2F_c^2)/3$.

2.3 Synthesis of Series 1 and 2

The ruthenium clusters Series **1a–2c** were prepared according to the Scheme 1, following four different methodologies, for further details see SI file. The numbers **1** and **2** refer to each series of analogous compounds; **a**, **b**, and **c** labels are used to indicate the three terminal alkynes used in the reactions.

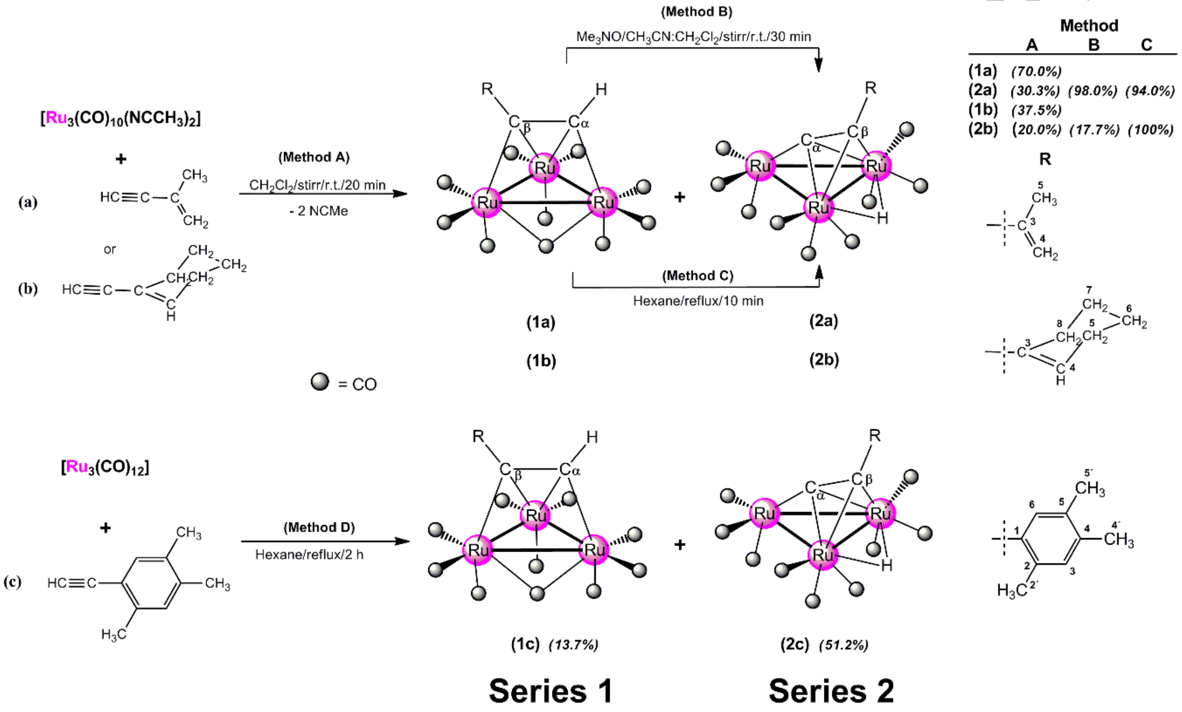

Scheme 1. Synthetic methods for the preparation of ruthenium clusters Series **1** and **2**.

2.4 Synthesis of Series 3 to 6

The *in situ* reaction of compounds **1a–1c** with the corresponding phosphine (PPh_3 or PPh_2Me), in a 1:1 stoichiometric ratio, gave the compounds in the Series **3** to **6**. The numbers **3**, **4**, **5**, and **6** refer to each series of analogous compounds; **a**, **b**, and **c** labels indicate the terminal alkyne, and the third number in the labels of Series **3** to **6** refers to the phosphine ligand used (1 for PPh_3; 2 for PPh_2Me). In Scheme 2 are summarized all the reactions carried out, for further details see SI file.

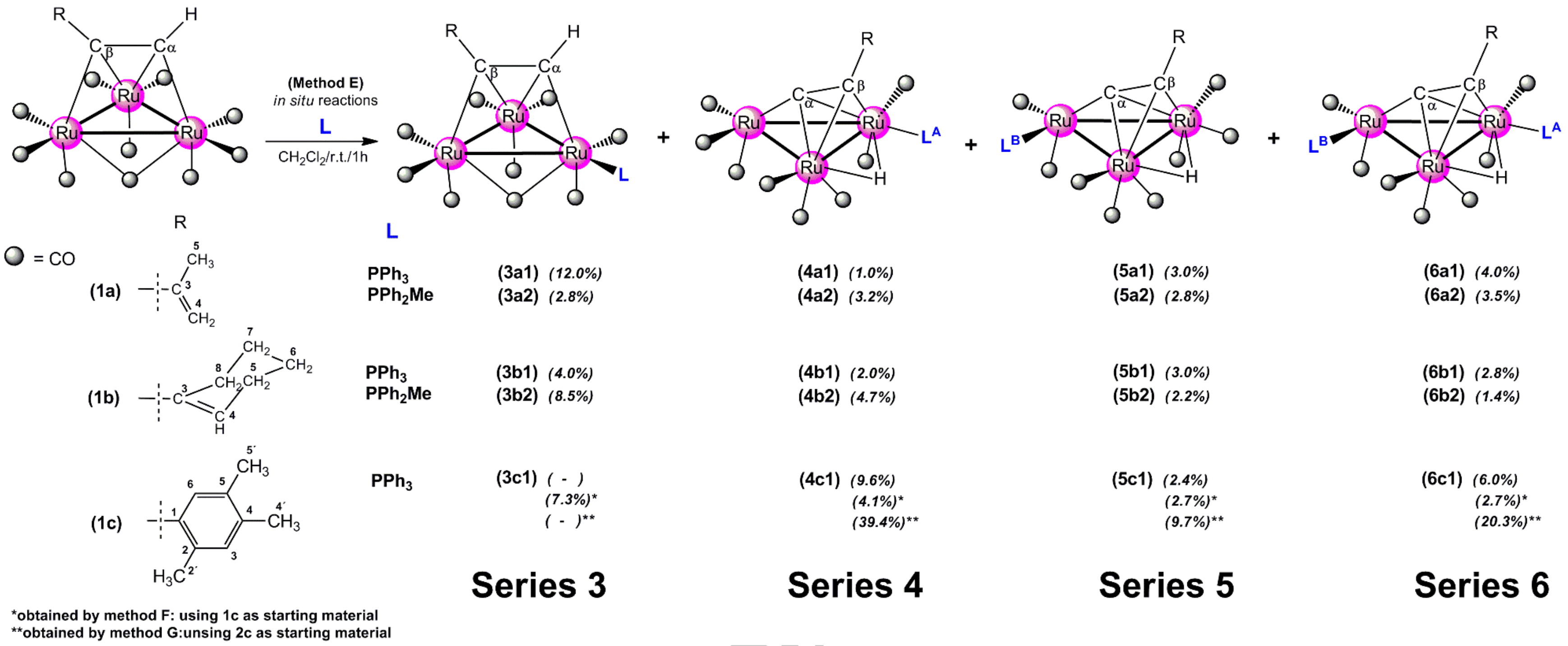

Scheme 2. Structures of mono- and bis-phosphine derivatives of acetylene and acetylide ruthenium clusters.

3. Results and discussion

Compounds **1a**, **2a**, **1b**, and **2b** were prepared following the traditional method by using the labile cluster $[Ru_3(CO)_{10}(NCMe_3)_2]$ in the presence of an excess of the terminal alkynes 2–methyl–1–buten–3–yne or 1–ethynylcyclohexene, respectively, at room temperature (See Scheme 1; Method A or experimental section in SI file for details). Two compounds were formed in each reaction, the parallel acetylene clusters of general formula $[Ru_3(\mu\text{–}CO)(CO)_9\{\mu_3\text{–}\eta^2\text{–}(//)\text{–}HC{\equiv}C\text{–}R\}]$ (**1a**: R = $C(Me){=}CH_2$; **1b**: R = $\overline{C{=}CH\text{–}(CH_2)_3\text{–}C}H_2$) were identified as the major products, whereas the acetylide compounds $[Ru_3(\mu\text{–}H)(CO)_9\{\mu_3\text{–}\eta^2\text{–}(\perp)\text{–}C{\equiv}C\text{–}R\}]$ (**2a**: R = $C(Me){=}CH_2$; **2b**: R = $\overline{C{=}CH\text{–}(CH_2)_3\text{–}C}H_2$) were the minor compounds.

The *in situ* reaction (See Scheme 2; Method E) of the corresponding parallel derivatives **1a** or **1b** with one equivalent of triphenylphosphine (PPh_3) or diphenylmethylphosphine (PPh_2Me) at room temperature for one hour yielded four different types of substituted compounds, which were assigned on the basis of ^1H and ^{31}P NMR solution studies and they will be discussed later. The carbonyl substitution reactions produced the analogous compounds $[Ru_3(\mu\text{–}CO)(CO)_8(L)\{\mu_3\text{–}\eta^2\text{–}(//)\text{–}HC{\equiv}C\text{–}R\}]$ (**3a1**: L = PPh_3, **3a2**: L = PPh_2Me, R = $C(Me){=}CH_2$; **3b1**: L = PPh_3, **3b2**: L = PPh_2Me, R = $\overline{C{=}CH\text{–}(CH_2)_3\text{–}C}H_2$). In these compounds, the phosphine ligand coordination takes place in the less hindered ruthenium atom having the Ru–C(σ) bond, maintaining the $\mu_3\text{–}\eta^2$ parallel coordination mode of the alkyne ligand to the metallic fragment. A second and a third type of compounds were also observed; they were identified as the perpendicular acetylide phosphine substituted isomers $[Ru_3(\mu\text{–}H)(CO)_8(L)\{\mu_3\text{–}\eta^2\text{–}(\perp)\text{–}C{\equiv}C\text{–}R\}]$ (**4a1** and **5a1**: L = PPh_3, **4a2** and **5a2**: L = PPh_2Me, R = $C(Me){=}CH_2$; **4b1** and **5b1**: L = PPh_3, **4b2** and **5b2**: L = PPh_2Me, R = $\overline{C{=}CH\text{–}}$

$\overline{(CH_2)_3\text{–}C}H_2$). Compounds **4a1**, **4b1**, **4a2**, and **4b2** have the coordinated phosphine attached to one of the metals having a Ru–C(π) bond (which would be considered the most crowded, but also the less electron rich metal site). On the other hand, compounds **5a1**, **5b1**, **5a2**, and **5b2** have the phosphine coordinated to the metal having the Ru–C(σ) bond (considered the less hindered and the electron richest metal site). All attempts to separate these sets of isomers were unsuccessful; the proportions for all isomeric pairs (for example, **4a1**:**5a1**) were estimated by ^1H NMR peak integration. The ratios were different in each case, and they depend of the used phosphine. For the PPh_3 derivatives, the proportions **4a1**:**5a1** and **4b1**:**5b1** were 25:75 and 40:60, respectively, being the major isomer the one that has the phosphine coordinated to the ruthenium atom with the C(σ) bond from the acetylene fragment. Reactions of perpendicular acetylide triruthenium clusters $[Ru_3(\mu\text{–}H)(CO)_9\{\mu_3\text{–}\eta^2\text{–}(\perp)\text{–}C\equiv C\text{–}R\}]$ with phosphine ligands gave exclusively compounds of type **5**, where the phosphine is coordinated to the less crowded ruthenium atom [10]. For the PPh_2Me derivatives, the ratios **4a2**:**5a2** and **4b2**:**5b2** were 54:48 and 68:32, respectively; these results contrast with the isomers ratio observed when L = PPh_3, where the major compound is the one with the phosphine coordinated to the ruthenium with the C(π) bond from the acetylene fragment. These results indicate that the more basic phosphine PPh_2Me is coordinated toward the less electron rich ruthenium (the most acidic metal) giving the major isomers **4a2** y **4b2**, and the higher steric hindrance of PPh_3 ligand favors the major isomers **5a1** and **5b1**.

The last compound formed in each carried out reaction were the disubstituted phosphine compounds $[Ru_3(\mu\text{–}H)(CO)_7(L)_2\{\mu_3\text{–}\eta^2\text{–}(\perp)\text{–}C\equiv C\text{–}R\}]$ (**6a1**: L = PPh_3, **6a2**: L = PPh_2Me, R = $C(Me){=}CH_2$; **6b1**: L = PPh_3, **6b2**: L = PPh_2Me, R = $\overline{C{=}CH\text{–}(CH_2)_3\text{–}C}H_2$) . In these complexes, the two phosphines are coordinated toward the two different types of ruthenium atoms present in the trimetallic cluster (Ru–C(σ) and Ru–C(π)).

In order to get a deeper insight in the course of these reactions, the following experiments were carried out. i) The pure parallel compounds $[Ru_3(\mu\text{–}CO)(CO)_9\{\mu_3\text{–}\eta^2\text{–}(//)\text{–}HC\equiv C\text{–}C(Me_3)=CH_2\}]$ (**1a**) or $[Ru_3(\mu\text{–}CO)(CO)_9\{\mu_3\text{–}\eta^2\text{–}(//)\text{–}HC\equiv C\text{–}\overline{C=CH\text{–}(CH_2)_3\text{–}CH}_2\}]$ (**1b**) reacts with PPh_3 in a 1:1 stoichiometric ratio in dichloromethane solution at room temperature for one hour to give the parallel derivative **3a1** or **3b1** in 44.5% or 30% yield as the only product. ii) On the other hand, compound **3a1** or **3b1** react with PPh_3 and Me_3NO in a 1:1:1 ratio to produce the isomers **4a1** and **5a1** in 25.8% yield overall, with a 29:71 ratio respectively, or **4b1** and **5b1** in 64.0% yield overall, with a 36:64 ratio respectively. In these reactions compound **3a1** was recovered in 13.3% and only traces of **3b1** were recuperated. In addition, compound **3a1** or **3b1** in the presence of one equivalent of Me_3NO (as decarbonylation reagent) did not undergo a skeletal rearrangement to produce the perpendicular derivatives (**4b1** or **5b1**). iii) The reactions of the isolated perpendicular derivative **2a** or **2b** with PPh_3 and Me_3NO also in a 1:1:1 ratio yielded the disubstituted derivative **6a1** or **6b1** in 15.6% and 14.9% yields respectively; it is interesting to note, that in the case of compound **2b** there was no evidence of **4b1** and **5b1** compound formation; however, reaction of **2a** formed compounds **4a1** and **5a1** in 28.8% yield overall, with a 22:78 ratio respectively.

These experimental results can suggest that the parallel compound **1a** or **1b** forms simultaneously in the *in situ* reactions, compound **3a1** or **3b1** and the perpendicular derivative **2a** or **2b** respectively. In addition, in two independent pathways, parallel monophosphine compound **3a1** or **3b1** continue to react with the phosphine in the presence of remaining Me_3NO, to give the monosubstituted isomers **4a1**:**5a1** or **4b1**:**5b1** respectively, meanwhile compound **2a** or **2b** also reacts with the phosphine to give the mixture of isomers **4a1**:**5a1** or **4b1**:**5b1**, but then again when time elapse these monophosphine compounds form the disubstituted compound **6a1** and **6b1**, respectively. These separated pathways are in agreement with the low yields obtained in these reactions by having competitive processes in compound formation.

In further studies, the reactivity of a ruthenium derivative having an aromatic group on the coordinated alkyne was also tested. The *in situ* reaction (See Scheme 2; Method E) of compound $[Ru_3(\mu–CO)(CO)_9\{\mu_3–\eta^2–(//)–HC\equiv C–C_6H_2–2,4,5–Me_3\}]$ (**1c**) with PPh_3 gave the isomeric compounds $[Ru_3(\mu–H)(CO)_8(PPh_3)\{\mu_3–\eta^2–(\perp)–C\equiv C–C_6H_2–2,4,5–Me_3\}]$ (**4c1** and **5c1**) in 12.0% yield. They were produced in an 80:20 ratio and all efforts to separate the mixture were unsuccessful. The disubstituted compound $[Ru_3(\mu–H)(CO)_7(PPh_3)_2\{\mu_3–\eta^2–(\perp)–C\equiv C–C_6H_2–2,4,5–Me_3\}]$ (**6c1**) was also formed in 6.0% yield. In these reaction, compounds $[Ru_3(\mu–CO)(CO)_9\{\mu_3–\eta^2–(//)–HC\equiv C–C_6H_2–2,4,5–Me_3\}]$ (**1c**) and $[Ru_3(\mu–H)(CO)_9\{\mu_3–\eta^2–(\perp)–C\equiv C–C_6H_2–2,4,5–Me_3\}]$ (**2c**) were also recuperated in 11.0 and 8.0 % yields respectively. The reactivity behavior of **1c** was different to the one observed for compounds **1a** or **1b**; in this case the analogous compound to **3a1** was not observed under these reaction conditions.

Compound **3c1** was obtained by changing the conditions (See Scheme 2; Method F). The reaction of the isolated parallel derivative **1c** with PPh_3 in a 1:1 stoichiometric ratio in dichloromethane at room temperature for 30 minutes, with the slowly addition of a trimetylamine *N*–oxide solution gave **3c1** in 7.3% yield, being the major product of the reaction. The isomer mixture **4c1**:**5c1** and the disubstituted product **6c1** were also formed in

6.8% and 2.7% yield respectively. This reaction mixture after 30 minutes showed a 60:20:7:13 ratio of compounds **3c1**, **4c1**, **5c1** and **6c1**, determined by ^{1}H NMR peak integration. Furthermore, when the mixture reaction was monitored by NMR in $CDCl_3$ solution for 12 hours the compounds ratio **3c1**, **4c1**, **5c1**, and **6c1** change to 27:47:8:18 respectively. These observations indicate that phosphine parallel derivative **3c1** easily transforms into the phosphine perpendicular derivative **4c1**, because of the high reactivity of compound **3c1**. Furthermore, the isomers ratio **4c1**:**5c1** change from 60:40 to 72:28, which is in agreement with the results obtained from the *in situ* reaction of compound **1c** with PPh_3 for 1 hour.

On the other hand, the reaction of isolated perpendicular cluster $[Ru_3(\mu–H)(CO)_9\{\mu_3–\eta^2–(\perp)–C\equiv C–C_6H_2–2,4,5–Me_3\}]$ (**2c**) with PPh_3 (See Scheme 2; Method G) in a 1:1 stoichiometric ratio in dichloromethane at room temperature for one hour gave the mixture of isomers **4c1** and **5c1** in 49.8% and compound **6c1** in 20.3% yield. Compound **2c** was also recovered in 18.2% yield in the reaction.

In general, it has been observed that PR_3 substitute CO ligands on the metallic centers σ–bounded to the organic moiety, as the M–C(π) bonds are usually directed toward the less electron rich metal [10,26,27]; however, the reactivity is ruled by the alkyne substituent.

In the cases that we have studied, a less bulky substituent on the terminal alkyne facilitate the formation of the acetylide isomers in the order: **5a1**>**5b1**>**5c1**, but it is also governed by the basicity and the steric hindrance of the phosphine used. Furthermore, phosphine parallel derivatives **3a1** and **3b1** are more stable than **3c1** derivative, which allow to isolate them. This higher stabilization can be achieved by using alkenyl substituents on the alkyne ligand, more than the use of an alkyne with a highly hindrance substituent and with different electronic properties as in an aromatic ring.

IR spectrums of the parallel derivatives of Series **1** and **3** displayed absorptions between 1870 and 1895 cm^{-1}, associated to the bridging carbonyl ligand (see SI file for full assignment). All spectra are very similar in the terminal carbonyl region. Compound Series **4**, **5** and **6** display only ν(CO) pattern in the terminal region, similar to those previously reported in analogous clusters [8].

The ^{1}H, ^{13}C{^{1}H} and ^{31}P{^{1}H} NMR spectroscopic data all compounds are summarized in the SI file. In the ^{1}H NMR spectra for compounds **1a** and **1b**, signals at high frequencies were found at 8.21 and 8.07 ppm, respectively, and were assigned to the hydrogen attached to the C_{α}–H. These signals are shifted to lower frequencies when compared to that observed in compound **1c** (8.44 ppm) [8], which indicates a nucleus protection by a major density in cluster **1c** than in **1a** or **1b**. The doublet resonances belonging to the C_{α}–H were found between 7.67 to 7.34 ppm in Series **3**, these signals are shifted to lower frequencies due to the phosphine coordination towards the ruthenium atom directly bonded to the C_{α}, which is consistent with a low σ character of the phosphine compared with the CO ligand.

The hydride signals for **2a** and **2b** were observed at −20.85 and −20.80 ppm respectively, the corresponding chemical shift of the hydride in compound **2c** was reported at −20.36 ppm [8] a rough tendency accordingly to the type of substituents on the acetylide, following the order: **2c**>**2a**≈**2b**. The chemical shifts at lower frequencies indicate that the electronic density decreases in the clusters with the presence of the alkenyl substituents.

The hydride signals in the ^{1}H NMR spectra of Series **4** were observed from −19.53 to −20.25 ppm, meanwhile the chemical shift for the hydride of Series **5** were found between −20.50

and −20.97 ppm. On the other hand, the resonances for the hydride ligands in Series **6** appeared from −19.77 to −20.38 ppm, observing similar tendencies when compared to the perpendicular acetylide cluster parent. They also showed parallel tendencies accordingly to the type of coordination of the phosphine toward the metal atom in the cluster: M−C_β(π) or M−C_α(σ) or when two Ru atoms are phosphine substituted. The hydride signal is shifted from higher to lower frequencies following the order: Series **4**>**6**>**5**. In addition, the chemical shifts of hydride ligands in compounds with PPh_3 as substituent appear at higher frequencies than those observed when a more basic phosphine (PPh_2Me) is used. The presence of different phosphines (PPh_3 or PPh_2Me) in comparable compounds, Series **4**, **5**, and **6**, causes a notable variation in the hydride chemical shifts (Δδ) regardless the type of coordinated acetylide: 0.32 ppm for **4a1** and **4a2**; 0.43 ppm for **4b1** and **4b2**; followed by those belonging to Series **6**: 0.23 ppm for **6a1** and **6a2**; 0.32 ppm for **6b1** and **6b2**, and finally Series **5** have the minor Δδ: 0.11 ppm for **5a1** and **5a2**; 0.16 ppm for **5b1** and **5b2**.

An analysis of the $\delta(C_\alpha)-\delta(C_\beta)$ and $\delta(C_\alpha)+\delta(C_\beta)$ of the *alpha* and *beta* carbon chemical shifts (see Table 1S in the SI file) was carried out for acetylene and acetylide compounds **1a**–**1c** (Series **1**), **2a**–**2c** (Series **2**), and for the PPh_3 derivatives of the Series **3**, **4**, **5** and **6**. The polarization of the C=C bond is associated to the $\delta(C_\alpha)-\delta(C_\beta)$, and the $\delta(C_\alpha)+\delta(C_\beta)$ have been proposed to be related to the total charge alteration in the C≡C triple bond [4,28,29]. Compounds **1a** and **1b** have $\delta(C_\alpha)-\delta(C_\beta)$ absolute values of 44.2 and 54.9 ppm, respectively, these values are larger than that reported for compound **1c** ($\delta(C_\alpha)-\delta(C_\beta)$ = 32.3 ppm) [8] and some other similar (//)–derivatives of general formula $[Ru_3(CO)_{10}(HCCR)]$ (R = substituted aryls), ($\delta(C_\alpha)-\delta(C_\beta)$ = 30.0 to 44.1 ppm) [8]. The value of **1b** is the second largest value reported for perpendicular alkynes triruthenium carbonyl derivatives, being the largest value the one obtained for the well–known compound [$Ru_3(CO)_{10}(HC{\equiv}C^tBu)$] ($\delta(C_\alpha)-\delta(C_\beta)$ = 56.9 ppm) [16]; both compounds have bulky and electrodonating alkyl groups directly attached to the triple bond. However, the analogous phosphine derivatives **3a1**, **3b1** and **3c1** have $\delta(C_\alpha)-\delta(C_\beta)$ values of 49.4, 58.4 and 50.5 ppm respectively. These large values indicate a larger polarization in the acetylene moiety when a phosphine ligand is attached to a ruthenium atom instead of a carbonyl group. Compound **1c** and its PPh_3 derivative **3c1** show the largest change in polarization going from 32.3 to 50.5 ppm with a $\Delta(\delta(C_\alpha)-\delta(C_\beta))$ of 18.2 ppm.

Compounds **2a** and **2b** have $\delta(C_\alpha)-\delta(C_\beta)$ values of 74.4 and 69.9 ppm, respectively; the value reported for compound **2c** is 78.6 ppm [8]. However, the values of the phosphine perpendicular derivatives (**4a1**, **4b1**, **4c1**; 81.8, 79.4, 84.4 ppm) are larger than those found for the parent perpendicular clusters. These values are higher than those for the isomeric compounds **5a1**, **5b1**, **5c1**; 79.5, 69.8, 73.6 ppm, indicating larger polarization over the triple bond when the phosphine is coordinated to the ruthenium atoms having Ru−C(π) bond. Also, the polarization in monosubstituted phosphine compounds is dependent of the substituent on the triple bond, following the order of the ligand: **a**<**b**<**c** with $\Delta(\delta(C_\alpha)-\delta(C_\beta))$ data of 2.3, 9.6, and 11.2 ppm, respectively. The values for the $\delta(C_\alpha)-\delta(C_\beta)$ of disubstituted cluster Series **6** are similar to the one found in Series **4** and **5**; however, there are no clear tendency in these values.

The analysis of the $\delta(C_\alpha)+\delta(C_\beta)$ of synthesized compounds indicate that the alkyne coordination mode, in a parallel fashion (with σ:σ:π interactions) to the metal core produce the largest charge alteration (315.2 to 334.5 ppm). On the other hand, the change in coordination, by breaking the C–H bond, with σ:π:π interactions, reduces this alteration

(259.2 to 269.3 ppm). In all phosphine derivatives, the tendency observed in charge alteration follows the order: Series **4**>**6**>**5**, which indicates that the coordination of a phosphine ligand in the ruthenium atom with a Ru−C(π) bond causes a higher change in triple bond charge than the coordination on a ruthenium with a Ru−C(σ) bond. There is certain tendency, in both charge alteration and bond polarization related to the electronic properties on the cluster, which increases by changing CO by PPh_3 ligands, in all type of alkyne ligands and coordination modes.

The $^{31}P\{^1H\}$ NMR data of parallel derivatives **3a1**–**3c1** have similar chemical shift between 40−45 ppm, while their analog compounds **3a2** and **3b2**, PPh_2Me derivatives, have the same chemical shift of 23.2 ppm. The chemical shifts of the Series **4** having a P−Ru−C(π) bond appears at lower frequencies than the Series **5** having a P−Ru−C(σ) bond in both PPh_3 or PPh_2Me cases. The δ $^{31}P\{^1H\}$ of the triphenylphosphine derivatives **4a1**−**4c1** are found between 35.6−36.3 ppm and the chemical shifts of the diphenylmethylphosphine derivatives **4a2** and **4b2** are in 14.3 and 15.3 ppm respectively. Meanwhile, the chemical shifts of compounds **5a1**−**5c1** are found between 50.9−54.9 ppm and the chemical shifts of the diphenylmethylphosphine derivatives **5a2** and **5b2** are in 35.6 and 35.4 ppm. Similar chemical shifts were found for the disubstituted PPh_3, compounds **6a1**–**6c1**. The signal multiplicity and coupling constants for both phosphorus atoms in these compounds were determined using heteronuclear irradiation experiments. The chemical shift of the phosphorus atom P^B attached to the ruthenium, with a C(σ) bond, is shifted to higher frequencies than the phosphorus atom P^A attached to the ruthenium, with C(π) bond, due to an increase in electron density around the metal center by the σ donation of the acetylide $C_α$.

3.1 X−Ray Diffraction Studies.

Suitable crystals of compounds **2b**, **3a1**, **3b1**, **4a1**, **4c1**, **6b1** and **6c1** for X−ray diffraction studies were obtained from slow evaporation of chloroform solutions at low temperature (5° C) for several days. Figs. 1–7 show the ORTEP diagrams, and selected bond distances and angles are summarized in Table 2. The results are in good agreement with the structures proposed in solution. The molecular structures obtained also allow us to confirm that, in general, the structural features are practically the same among isostructural acetylide (**2b**, **4a1**, **4c1**, **6b1** and **6c1**) or acetylene (**3a1** and **3b1**) complexes, respectively. Compound **2b** displays a positional disorder due to two different conformations in the cyclohexenyl ring, an envelope and a fairly planar type conformations with 50−50 % probability were found, as shown in Fig 1b.

Table 2. Selected bond lengths (Å) and angles (°) of compounds **2b**, **3a1**, **3b1**, **4a1**, **4c1** and **6b1**.

Compound	2b	3a1	3b1	4a1	4c1	6b1
Bond lengths						
Ru(1)–Ru(2)	2.7909(3)	2.855(1)	2.8445(4)	2.8149(6)	2.8160(4)	2.8090(6)
Ru(2)–Ru(3)	2.7970(2)	2.703(1)	2.6993(5)	2.8042(5)	2.8031(4)	2.8106(6)
Ru(3)–Ru(1)	2.8267(3)	2.790(2)	2.7538(5)	2.8154(5)	2.8087(4)	2.8639(5)
Ru(1)–P(1)	−	2.368(3)	2.3710(1)	2.3630(1)	2.3730(9)	2.3675(13)
Ru(3)–P(2)	−	−	−	−	−	2.3277(14)
C(1)–C(2)	1.326(3)	1.39(2)	1.405(5)	1.319(6)	1.304(4)	1.322(8)
C(2)–C(3)	1.398(10)a* 1.399(10)b*	1.52 (2)	1.489(5)	1.450(6)	1.464(4)	1.464(8)
C(3)–C(4)	1.506(6)a*	1.33(3)	1.335(6)	1.363(7)	1.403(4)	1.372(10)

	1.322(7)b*					
Ru(1)–C(1)	2.203(2)	2.10(1)	2.108(4)	2.184(5)	2.187(3)	2.163(5)
Ru(1)–C(2)	2.249(13)	−	−	2.278(5)	2.323(3)	2.256(5)
Ru(2)–C(1)	2.200(2)	−	−	2.216(5)	2.206(3)	2.226(5)
Ru(2)–C(2)	2.306(14)	2.08(1)	2.101(4)	2.261(5)	2.269(3)	2.251(6)
Ru(3)–C(1)	1.944(2)	2.19(2)	2.191(5)	1.952(4)	1.948(3)	1.946(5)
Ru(3)–C(2)	−	2.29(1)	2.283(4)	−	−	−
Bond angles						
Ru(1)–Ru(2)–Ru(3)	60.778(7)	60.23(4)	59.498(1)	60.139(1)	59.979(10)	61.277(14)
Ru(2)–Ru(3)–Ru(1)	59.505(6)	62.52(4)	62.876(1)	60.122(1)	60.239(10)	59.335(14)
Ru(3)–Ru(1)–Ru(2)	59.718(7)	57.25(3)	57.626(1)	59.739(1)	59.782(10)	59.388(14)
Ru(2)–Ru(1)–P(1)	−	142.21(9)	137.61(3)	111.22(3)	110.14(3)	110.48(4)
Ru(3)–Ru(1)–P(1)	−	132.96(9)	131.98(3)	168.85(3)	169.91(3)	168.49(4)
Ru(1)–Ru(3)–P(2)	−	−	−	−	−	107.71(4)
Ru(2) −Ru(3)–P(2)	−	−	−	−	−	161.32(4)
Ru(3)–C(1)–C(2)	155.41(17)	76.2(8)	75.3(2)	154.6(4)	156.7(3)	155.3(5)
Ru(1)–C(1)–C(2)	74.58(12)	111.2(9)	112.8(3)	76.7(3)	79.10(2)	76.5(4)
Ru(2)–C(2)–C(1)	77.30(11)	109.2(9)	107.1(3)	71.0(3)	70.50(2)	71.7(4)
C(1)–C(2)–C(3)	139.51(18)a*	121.4(12)	122.7(4)	140.1(5)	144.2(3)	139.2(6)
	145.35(18)b*					
Interline and interplane angles						
C(1)–C(2)/Ru(1)–Ru(2)	89.0(2)	6.7(8)	−3.8(2)	88.3(3)	87.8(3)	87.7(5)
C(1)–C(2)/Ru(1)–Ru(2)–Ru(3)	18.9(2)	3.2(8)	3.1(2)	18.4(3)	20.6(3)	18.8(5)
P(1)–Ru(1)/Ru(1)–Ru(2)–Ru(3)	−	32.2(5)	36.2(4)	−6.8(4)	−0.5(4)	−5.7(6)
P(2)–Ru(3)/Ru(1)–Ru(2)–Ru(3)	−	−	−	−	−	14.1(6)

Ru(1)–Ru(2)–C(11)/Ru(1)–Ru(2)–Ru(3)	–	22.3(5)	15.2(4)	–	–	–

*The a and b labels are due to positional (conformational) disorder of the cyclohexenyl ring

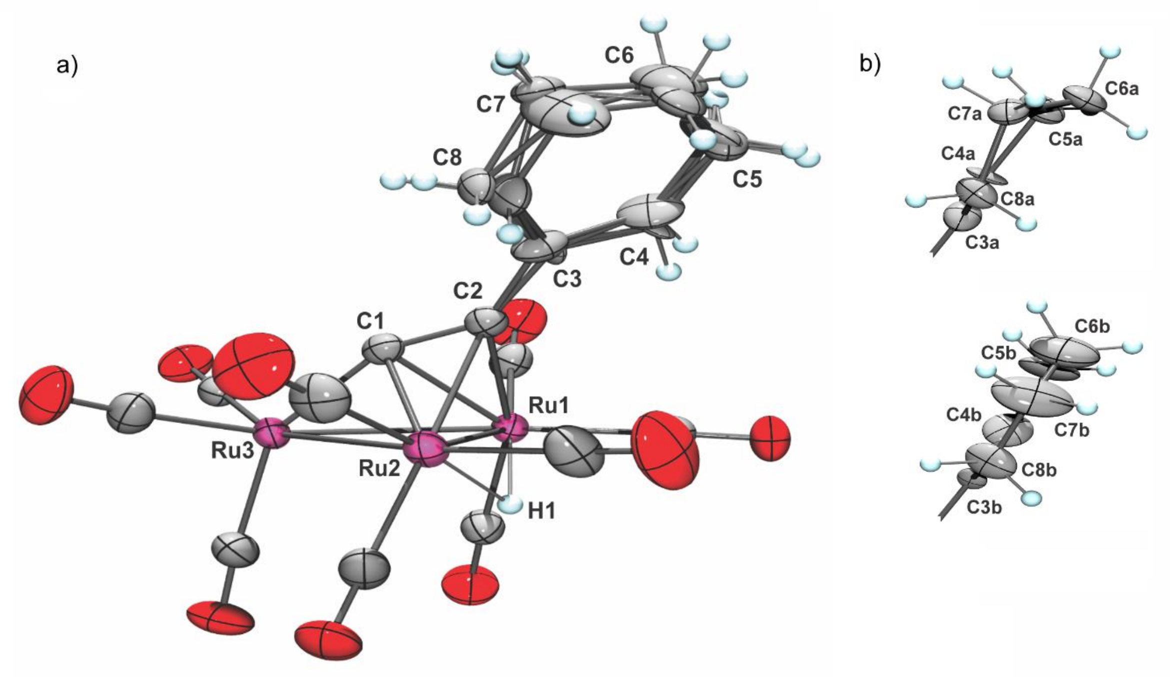

Fig. 1.a) ORTEP view of compound **2b** (30% probability). b) Envelope and planar conformations of the cyclohexenyl ring.

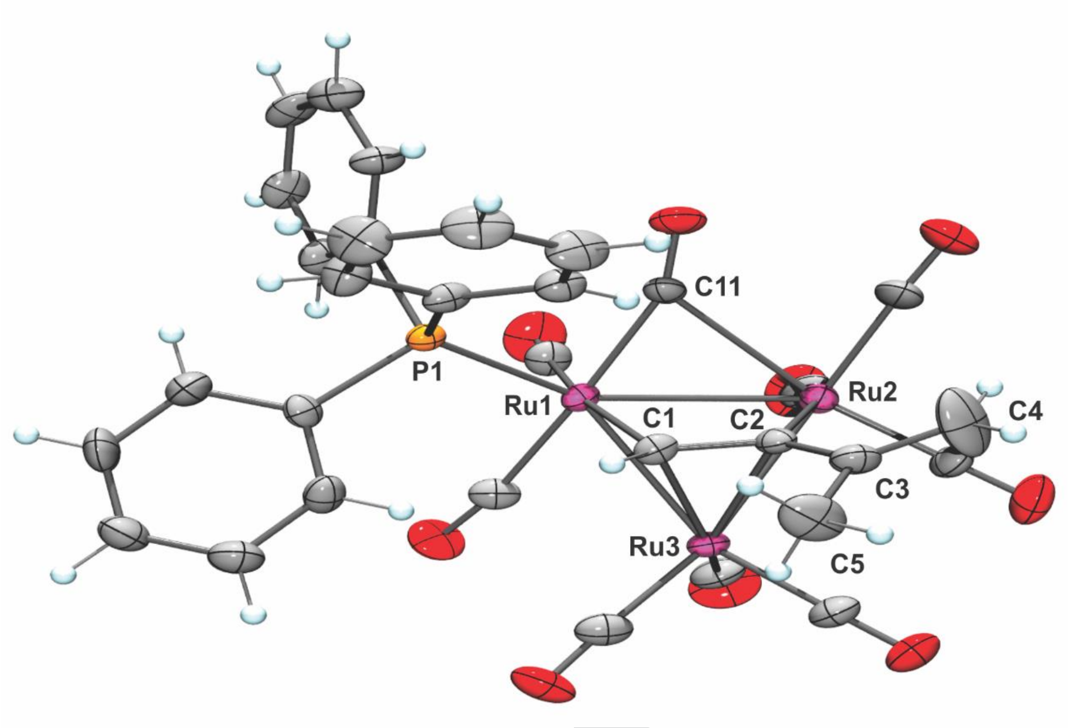

Fig. 2. ORTEP view of compound **3a1** (30% probability).

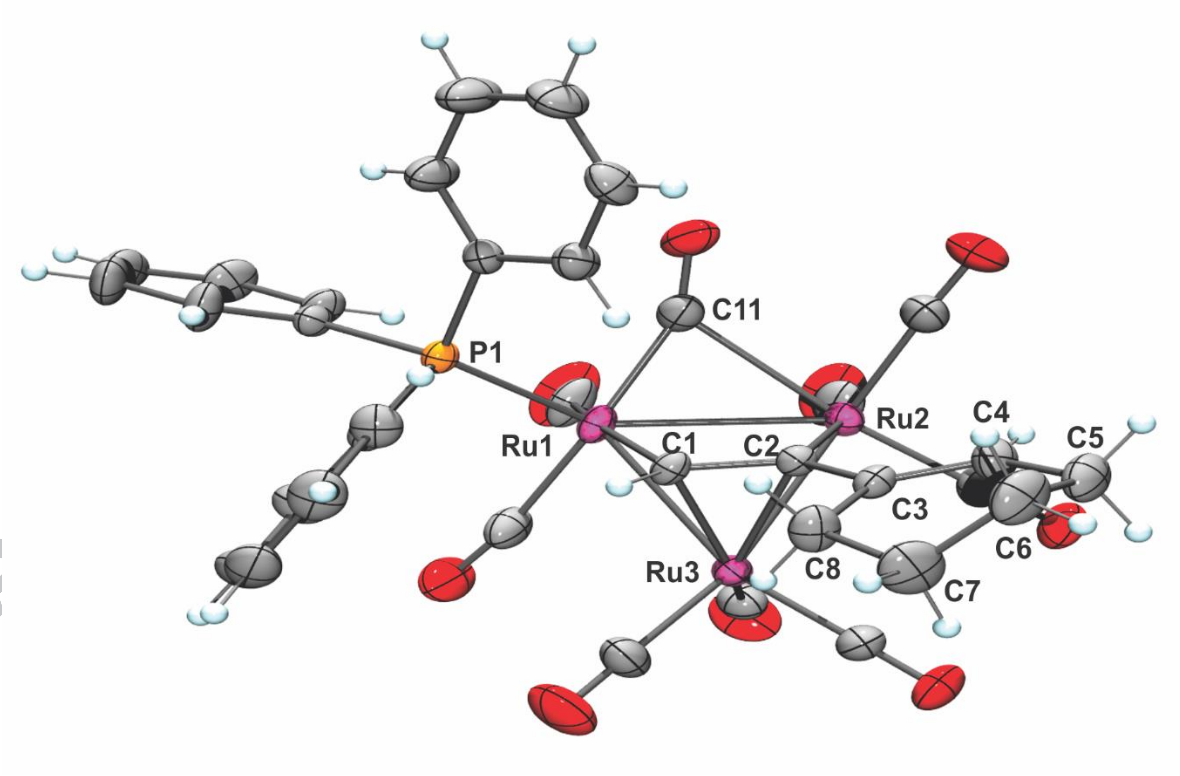

Fig. 3. ORTEP view of compound **3b1** (30% probability).

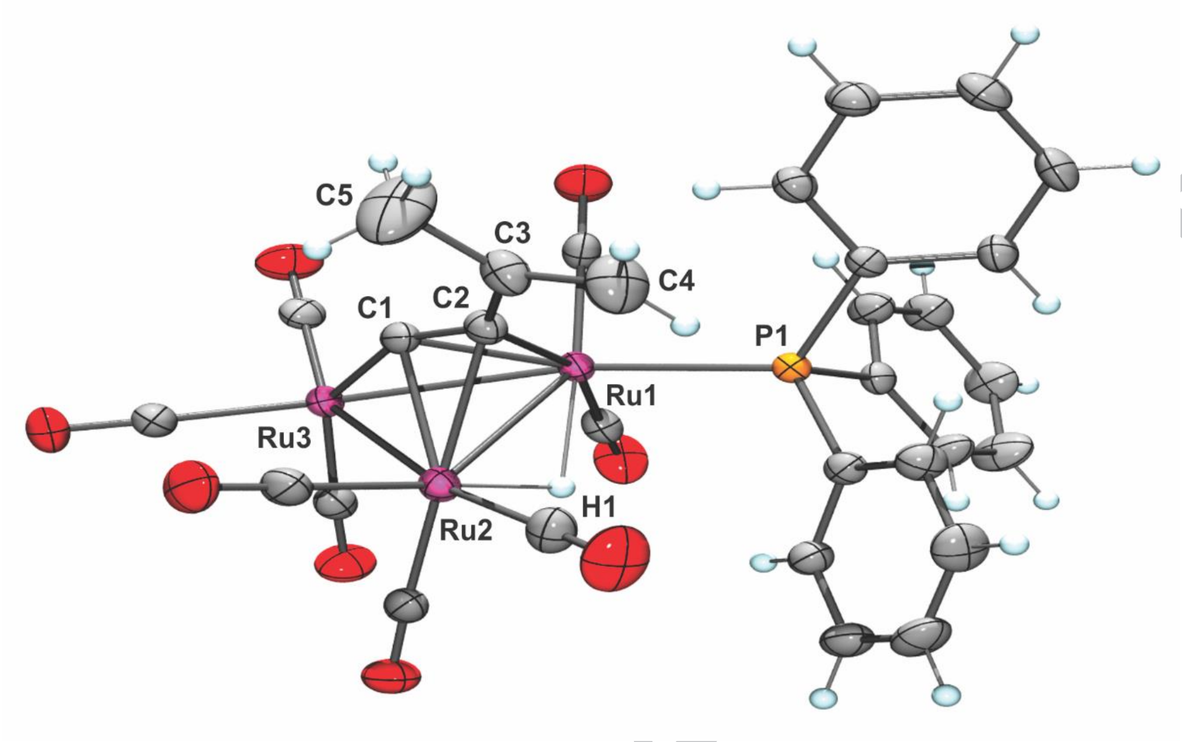

Fig. 4. ORTEP view of compound **4a1** (30% probability).

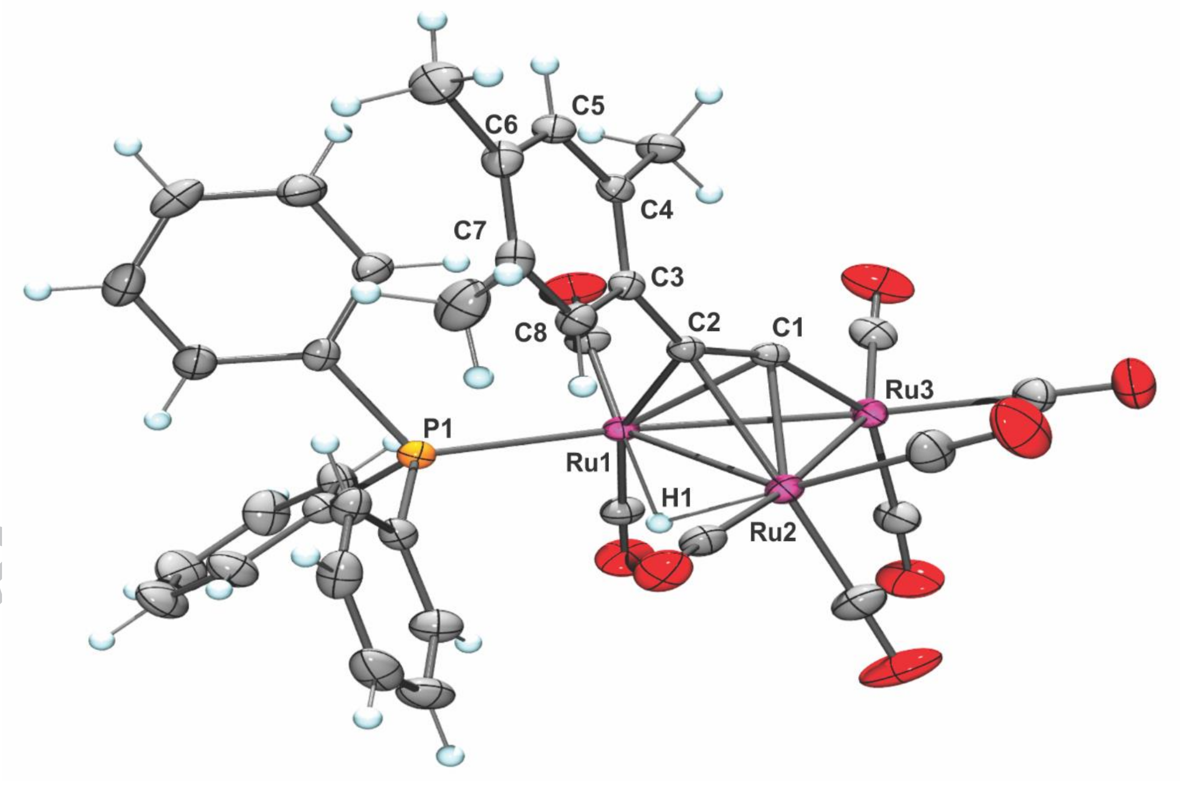

Fig. 5. ORTEP view of compound **4c1** (30% probability).

The metal–metal distances in compound **2b** are similar among them, even though one is larger than the other two, due to a slightly asymmetric coordination of the acetylide ligand on the triangular face of the cluster. This asymmetry increases when one or two phosphine ligands are attached to the trinuclear clusters, generating larger distances from Ru(1) to the other two metals in compounds **4a1** and **4c1**. In the case of compound **6b1** (Fig. 6), the substitution of both PPh_3 are confirmed to occurred in different metal centers, creating the largest Ru–Ru bond (2.8639(5) Å) between the metal atoms who bear the phosphines. The poor quality of the crystals for **6c1** [30] only permits sketch the connectivity of the heavy atoms in the structure of this compound (Fig. 7); although, its study allowed us to identify differences in the two coordinated phosphorous when compared to compound **6b1**.

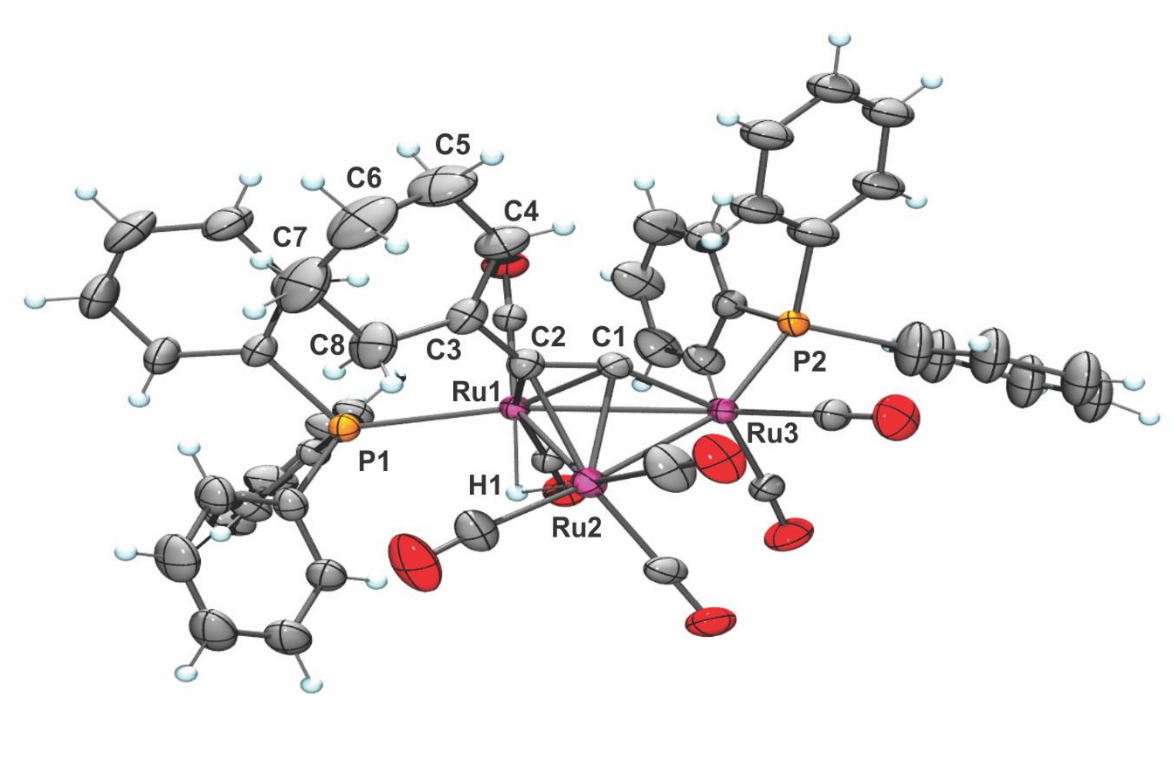

Fig. 6. ORTEP view of compound **6b1** (30% probability).

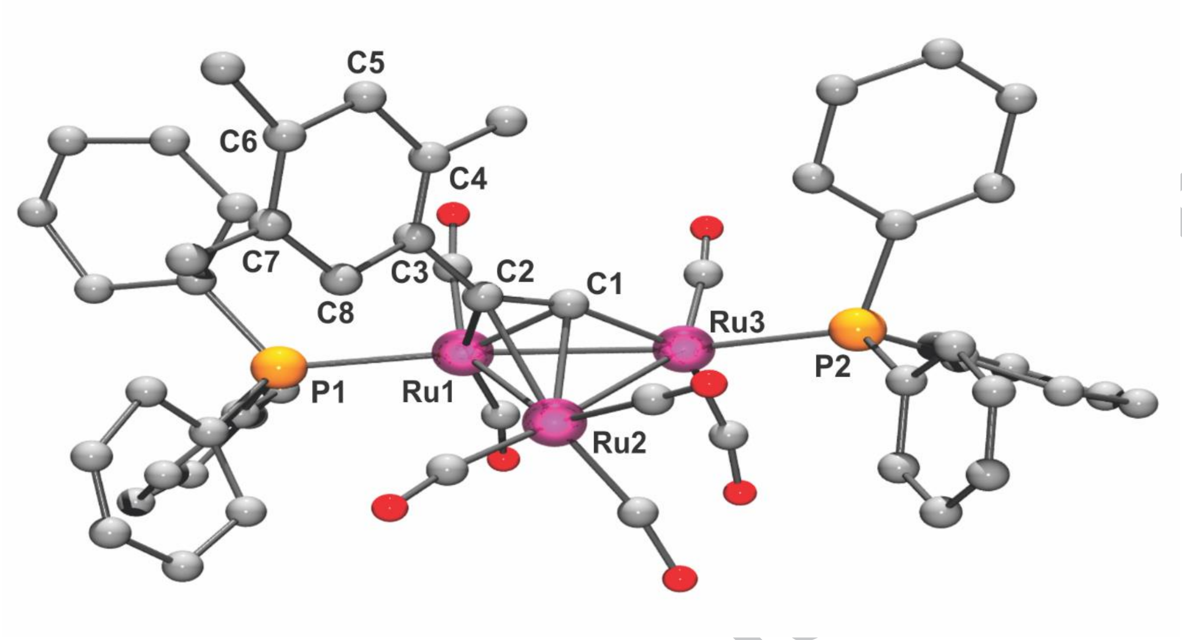

Fig. 7. Molecular structure of compound **6c1**.

The structures of compounds **2b**, **4a1**, **4c1** and **6b1** show the perpendicular coordination of the corresponding acetylide group. The cyclohexenyl group in compound **6b1** shows an envelope ring conformation. The Ru−Ru distances are slightly larger when phosphine ligands are coordinated to the metal framework than those in the CO derivative, changing the M−M distances from 2.805 Å (av) in **2b** to 2.810 (av) Å in monophosphine compounds **4a1**, **4c1**, or to 2.816 (av) Å in all substituted compounds **4a1**–**6b1**. These data indicate that neither changes in electronic nor steric properties caused by the phosphine substitution are present, leaving almost unaffected the metallic structure in the clusters.

The Ru(1)−P(1) bond distances with only π interaction with both acetylide carbons are similar to each other in compounds **4a1**−**6b1**. They are larger (2.3678 (av) Å) than the Ru(3)–P(2) bond distance (2.3277(14) Å), where the C(1) of the acetylide is σ coordinated to the metal atom. Apparently, this interaction shortens the P−Ru coordination; a similar trend has also been reported in some other trinuclear ruthenium acetylide diphosphine clusters [8].

The C(1)−C(2) bond distances are similar for all acetylide complexes, ranging from 1.304(4) Å in **4c1** to 1.322(8) Å in **6b1**, and they are similar to several other acetylide−ruthenium trinuclear clusters [8]. These distances are close to the normal C=C double bond distance (C_{sp2}–C_{sp2} 1.34 Å [31]) reflecting the change in hybridization of these carbons upon coordination; thus it can be observed that the bond distance increases in the order **4c1**<**2b**<**4a1**<**6b1**, which is usually related to the polarization in the C–C bond of the coordinated acetylide [8].

The Ru(3)–C(1)–C(2) angles of the acetylide clusters are in the 154.6(4)–156.7(3)° range, while the C(1)–C(2)–C(3) angles are smaller (139.2(6)–144.2(3)°). In compound **2b** there is a significant difference in this angle, 139.51(18)° for C(3a) or 145.35(18)° for C(3b), that is related to the disorder around the cyclohexenyl ring where two different conformations were found. The C(1)–C(2)–C(3) angles increase according to **6b1**(139.2(6)°)<**4a1**(140.1(4)°)<**2b**(139.51(18)°)<**4c1**(144.2(3)°); this trend can be associated with a decrease in repulsive steric interactions between the alkenyl fragments and the phenyl rings in the PPh_3 ligands. In the case of **2b**, the preferred rotational orientation of the cyclohexenyl ring increases the repulsive forces with the CO groups, while for **4c1**, the presence of the substituted phenyl ring and its planarity find a better way to be spatially distributed. Compound **6b1**, being the most crowded complex and having a cyclohexenyl substituent and two PPh_3 ligands, has the shortest angle; however, the resemblance of values confirms that the only important contacts that affect this structural parameters are due to the interactions of the acetylide functional groups and the phosphine coordinated to Ru(1) atom.

The angles formed by the C(1)–C(2) vector and the plane formed by the three metal atoms in the acetylide compounds have different values (18.4(6)–20.6(2)°); the order observed was **4a1<6b1≈2b<4c1**. It is worth to mention that complexes coordinated to ene–yne type ligands have smaller values (18.7° av) than that of the trimethylphenyl aromatic ring (20.6(2)°), this situation is also associated with the inherent hindrance properties of the ligands and its spatial distributions.

The type of substituents on C(2) does not significantly affects the perpendicular relationship between the C(1)–C(2) and Ru(1)–Ru(2) vectors, these interlinear angles are found in the 87.7(3)–89.0(2)° range (**6b1<4c1<4a1<2b**) with an average of 88.2°. This value is slightly smaller than those reported for the analogous acetylide compounds with the absence of a coordinated phosphine, $[Ru_3(\mu\text{–}H)(CO)_9(\mu_3\text{–}\eta^2\text{–}(\perp)\text{–}C{\equiv}C\text{–}R\}]$ (R = $SiMe_3$, 89.7°; $SiPh_3$, 89.81°) [28].

For the acetylide phosphine substituted compounds, the P(1) are roughly located below the plane of the metal atoms (opposite to the acetylide fragment) [P(1)/triangular plane distance: 0.020 Å, **4c1**; 0.234 Å, **6b1**; 0.278 Å, **4a1**], with angles P(1)–Ru(1)/Ru(1)–Ru(2)–Ru(3) of −0.5(4)°, −5.7(6)°, −6.8(4)°, respectively. However, the P(2) in complex **6b1** is located above the metal triangle plane (0.566 Å), with an angle P(1)–Ru(1)/Ru(1)–Ru(2)–Ru(3) of 14.1(6)°. As it has been mentioned, there are differences in the orientation of the coordination of both P atoms in compounds **6b1** and **6c1**. The analysis of both structures showed, that in **6b1** both P atoms are in the same side of an imaginary perpendicular plane bisecting the triangular Ru plane, indicating that the phosphine ligands are found in a *cisoid* position to each other (see Fig. 6); while in **6c1**, the two P atoms are located in *transoid* position, (see Fig. 7). These two different structures were proposed to coexist in equilibrium in solution for the reported compound $[Ru_3(\mu–H)(CO)_7(PPh_3)_2(\mu_3–\eta^2–(\perp)–C\equiv C–{}^tBu)]$[10]; however, in our case, we have no evidence that this type of behavior is present in the bistriphenylphosphine substituted complexes at room temperature.

It is worth to notice that in the last two decades, it has only been reported 21 structures of analogs to compound **2b**, **4a1**, **4c1** or **6b1** accordingly to the CCDC database, having the general formula $[Ru_3(\mu–H)(CO)_{9-2x}(LL)_x(\mu_3–\eta^2–(\perp)–C\equiv C–R\}]$ (when $x = 0$, R = alkyl [26,27,32,33], aryl [8,34], SiR_3 [35-38], and Fp = $(\eta^5\text{-}C_5H_5)Fe(CO)_2$ [39]); when $x = 1$, LL = diphosphine, R = alkyl [33,40] and R = aryl, [8,41-43]). Among them, there is no structure described that has two monophosphines coordinated in two different ruthenium atoms, similar to compound **6b1**. In a comparative analysis, it was found that the distances C(1)–C(2) previously reported are in the range of 1.29(1)–1.327(5) Å, and there is no tendency in these values that can be directly associated to the R substituent (alkyl, aryl or silyl) attach to the acetilyde fragment. However, Akita and coworker [39] have reported the only structure of a compound where there is a metallic atom directly attach to the acetylide fragment: $[Ru_3(\mu–H)(CO)_9(\mu_3–\eta^2–(\perp)–C\equiv C–Fp\}]$ Fp = $(\eta^5\text{-}C_5H_5)Fe(CO)_2$. In this structure, the C(1)–C(2) bond is one of the most elongated upon coordination, consequently is the largest distance reported (1.33(2) Å). Also, in this compound the Ru(3)–C(1)–C(2) angle of 159(1)° is the largest reported. In general, the Ru(3)–C(1)–C(2) angle in ruthenium diphosphine clusters have values between 150.6(1) and 156.3(3)°, with **4c1** having the second largest value (156.7(3)°) reported. This range is smaller than the values found for the Ru(3)–C(1)–C(2) angle in ruthenium carbonyl silyl-acetylide clusters of 152.0(3) to 157.8(6)°, the increase is due to the hindrance properties of the acetylide silyl substituents.

From the same data, the Ru(1)–Ru(2) bonds bridged by the hydride ligand, in clusters with coordinated phosphines, have values between 2.7725(6) and 2.8149(6) Å; compound **6b1** has the largest value (2.8160(4) Å) reported. For carbonyl clusters the Ru(1)–Ru(2) distances were found between 2.7887(3) and 2.819(2) Å, cluster **2b** has one of the smallest values (2.7909(3) Å) and compound [$Ru_3(\mu–H)(CO)_9(\mu_3–\eta^2–(\perp)–C\equiv C–Fp\}$] [39] the largest.

When a diphosphine (LL) is coordinated to two different ruthenium atoms (C(π) and C(σ) bonded toward the metallic fragment), the distances for Ru(1)–P(1) and Ru(2)–P(2) were found between 2.2990(5)–2.3730(9) and 2.282(1)–2.3277(14) Å respectively. In compounds reported here, **4a1**, **4c1** and **6c1**, the Ru–P distances have the largest values, these can be attributed to the fact that they have two coordinated monophosphines, and there are more degrees of freedom compared with the bridged diphosphine derivatives reported elsewhere.

In the case of the parallel acetylene derivatives **3a1** and **3b1**, the three metal–metal distances are significantly different to each other; the Ru(1)–Ru(2) axis parallel to the acetylene vector C(1)–C(2), which also has a bridging CO group, is the largest, 2.8479 Å (av). The Ru(3)–Ru(1) bond being the second largest, 2.7719 Å (av), is the one that involved the phosphine coordination around Ru(1). Thus, the presence of the coordinated ligands (acetylene, phosphine and bridged CO), distorts considerably the metal triangle, confirmed by the three different bond angles around each metal center.

From the molecular structure, it can be observed that the CO substitution by the phosphine ligand took place in the ruthenium that is the least hindered center, having the H substituent atom in the acetylene carbon. The Ru–P bond distances are similar to each other, 2.3695 Å (av), and are also very similar to those Ru(1)–P(1) found in the acetylide complexes, 2.3678 Å (av); apparently, the σ interaction from the CH acetylene group has no influence in the

Ru−P interaction. The C(1)–C(2) bond distances are similar for both acetylene complexes, 1.396 Å (av), and they are larger than the C–C acetylide distances here reported, 1.315 Å (av). The acetylene distances are larger than the normal C=C double bond distance reflecting greater changes in hybridization and polarization of these carbons upon coordination when compared with the acetylide complexes.

The C(1)–C(2)–C(3) angles are similar for compounds **3a1** and **3b1**, 122.1° (av), and are shorter than the bond angles found in the acetylide complexes, 141.2° (av). These data confirm significant changes in carbon hybridization, the acetylene carbons have more sp^3 character, while the acetylide carbons have more sp^2 character. These can be related to the coordination mode of the alkyne type derivatives, in the parallel acetylene coordination there are two σ and one π interactions with the metal framework, meanwhile in the acetylide complexes there is one σ and two π interactions with a concomitant C−H bond breaking. Thus, the carbon atoms changed from a sp hybridization in the alkyne free ligand to a more sp^3 resemble character in the parallel acetylene, returning to a close sp^2 hybridization in the perpendicular acetylide.

The angles formed by the C(1)–C(2) vector and the plane of the three metal atoms in the acetylene clusters are closely parallel to each other, 3.1° (av), where the acetylene carbon with an alkene substituent is slightly farther away from the metal triangle, as expected. The steric effects of the propenyl or the cyclohexenyl groups also have influence in the small distortion between the C(1)–C(2) and the Ru(1)–Ru(2) vectors, showing angles of 6.7° for **3a1** and −3.8° for **3b1**; the negative sign indicates that the C(2)–(cyclohexenyl) is pointing away from the center of the Ru triangle relative to the Ru(1)–Ru(2) axis.

For these compounds, the P(1) is located above the plane of the metal atoms (in the same side of the acetylene fragment), a different situation when compared to those in the acetylide complexes. [P(1)/triangular plane distance: 1.262 Å, **3a1**; 1.402 Å, **3b1**], with angles P(1)–Ru(1)/Ru(1)–Ru(2)–Ru(3) of 32.2(5)°, 36.2(4)°, respectively.

The bridged carbonyl in both compounds is also located above the plane of the ruthenium atoms, in the same side of the other two coordinated ligands. With a C(11)/triangular plane distance of 0.666 Å in **3a1** and 0.441Å in **3b1**, and with Ru(1)–Ru(2)–C(11)/Ru(1)–Ru(2)–Ru(3) angles of 22.3(5)°, 15.2(4)°, respectively. The difference can be attributed to the interaction with the substituents of the phosphorous and the acetylene fragment, and these also asymmetrically distort the Ru–C(11) (μ–CO) distances making them significantly different in each complex: Ru(1)–C(11) of 2.002(14) and C(11)–Ru(2) of 2.574(14) Å in **3a1** and Ru(1)–C(11) of 1.957(6) Å and C(11)–Ru(2) of 2.493(5) Å in **3b1**. Apparently, electronic factors of the coordinated P in Ru(1) shorten the Ru(1)–C(11) bond.

To the best of our knowledge, there is only one similar structure to compounds **3a1** and **3b1** recently described in the crystallographic database, belonging to compound $[Ru_3(\mu\text{–}CO)(CO)_8(P(^iPr)_3)\{\mu_3\text{–}\eta^2\text{–}(//)\text{–}HC\equiv C\text{–}^tBu\}]$ [44]. This compound has also the same asymmetric distribution of the bridge carbonyl with Ru–C(μ–CO) distances of 2.096(5) and 2.475(4). Besides, the C(1)–C(2) distance of 1.384(5) Å is similar to the one found in compound **3a1** (1. 39(2) Å) but is shorter than the bond observed in compound **3b1** (1.405(5) Å), probably due to a higher steric hindrance of the alkyne substituent in the former compound. It has been recently described that the molecular structure of the parallel acetylene cluster $[Ru_3(\mu\text{–}CO)(CO)_9\{\mu_3\text{–}\eta^2\text{–}(//)\text{–}(Ph\text{–}C\equiv C\text{–}2\text{–}MeCOO\text{–}Ph)\}]$ [45], with a non−terminal acetylene coordinated, has also an asymmetric distribution of the bridge CO ligand, with Ru–C(μ–CO) distances of 2.029(2) and 2.337(2) Å, and with a C(1)–C(2) distance of 1.396(3) Å. In the case of compounds described here, these asymmetries are confirmed to be related due to the influence of both hindered acetylene and phosphine substituents.

A thoroughly search in the CCDC data base showed that in the last two decades there was only described seven structures of carbonyl clusters with a parallel acetylene ligand coordinated of general formula [Ru_3(μ–CO)$(CO)_9${μ_3–η^2–(//)–(R–C≡C–R´)}], when R = H, R = alkyl [28,40], R = R´ = alkyl [40] and R = alkyl, R´= aryl [45,46], and there is only one structure with two monophosphines coordinated to the ruthenium atoms who have both C(σ) bonds [Ru_3(μ–CO)$(CO)_7$$(PPhMe)_2${$\mu_3$–$\eta^2$–(//)–(R–C≡C–R´)}], R = R´ = alkyl, and it was described by Bruce and coworkers in 1991 [9], and there is another structure having a diphosphine (dppm) asymmetrically coordinated, reported in 1997 [11].

For those reported compounds, the distances C(1)–C(2) were found between 1.378(5) and 1.412(2) Å, compounds **3a1** and **3b1** have distances that fall in the same range, and they are smaller than the normal C–C single bond distance (C_{sp3}–C_{sp3} 1.54 Å [31]).

Also, the Ru(1)–Ru(2) distances, having the μ–CO, are the largest distances with values between 2.8131(9) and 2.866(1) Å, regardless if they have a phosphine or carbonyl ligands attached. However, the Ru(3)–Ru(1) distance for compound **3a1** is the largest with a value of 2.790(2) Å, while the reported distances for all other parallel derivatives were found in the range 2.698(1)–2.794(1) Å, consequently the Ru(2)–Ru(3) distance in compounds **3a1** is one of the small distances (2.703(1) Å), all other compounds have distances between 2.6993(5) and 2.7548(5). The Ru(1)–P(1) distances in all parallel acetylenes have values between 2.347(2) and 2.371(1) Å, they are similar to those reported here for perpendicular derivatives.

The dihedral angle Ru(1)–Ru(2)–C(2)–C(1) for compounds **3a1** and **3b1** have values of 5.59 and 3.80°, meanwhile the reported compounds have values between 7.12 and 0.32°, being the smallest (less than 1.0°), those belonging to highly symmetric compounds. The values found in compounds reported here are in agreement with fact that they are terminal alkynes. Finally, one of the fewest molecular structures described having a ‘‘parallel’’ ene–yne acetylene substituent ruthenium cluster belongs to compound $[Ru_3(\mu–H)_2(CO)_9\{\mu_3–\eta^2–(//)–(CH_2=C(H)–C\equiv C–C(=O)OMe)\}]$ [47]. In this complex the C(1)–C(2) distance of 1.372(11) Å for molecule A and 1.383(11) Å for molecule B are slightly shorter than the one observed in the monophosphine derivatives. Is worth to notice that this cluster has two bridge hydride ligands instead of a bridging carbonyl ligand.

4. Conclusions

Six series of parallel acetylene and perpendicular acetylide ruthenium trinuclear carbonyl and phosphine clusters were synthesized. The use of different synthetic strategies allowed to obtain twenty new phosphine substituted clusters. The $^{13}C\{^1H\}$ NMR chemical shifts of C_α and C_β, and their corresponding sums and subtractions reflect the change in polarization or charge on the triple bond. In our studies, we found that in all phosphine perpendicular acetylide derivatives the charge alteration follows the order Series **4**>**6**>**5** due to the coordination of the phosphine ligand toward the ruthenium with a Ru−C(π) bond rather than the coordination on a ruthenium with a Ru−C(σ) bond. The well−known low stability of acetylene compounds with a π:π:σ ligand donation was modified by the presence of a phosphine ligand. These played an important role to stabilize the less thermodynamically stable $\mu_3–\eta^2–(//)$ parallel acetylene coordination mode, especially for terminal alkynes, and determine the molecular structures of compounds **3a1** and **3b1** in the solid state. The solid state structures of compounds **2b**, **4a1, 4c1** and **6b1** showed no significant changes in structural parameters, having the μ_3–η^2–(⊥) perpendicular acetylide coordination mode.

Acknowledgements

This work has been partially supported by projects of Consejo Nacional de Ciencia y Tecnología (CONACYT) Mexico, Grants: No.CB2011/169067. Cátedras 2016/222. ‘‘Integración de Redes Temáticas de Colaboración Académica 2015 SEP/PRODEP: Química Organometálica y Catálisis” and PAI−UAEH−2015 No. 3289 and 3313. We appreciate the support given. Additionally, AIML, EGRG and DOGA thank CONACYT for their scholarships. We also wish to acknowledge Irais Gómez, Angélica Cerón, Alexandra Ferreira, and Viridiana Juárez for their lab work.

Appendix A. Supplementary data

CCDC 1869108, 1868967, 1869110, 1869109, 1868968, and 1868969 contain the supplementary crystallographic data for compounds **2b**, **3a1**, **3b1**, **4a1**, **4c1** and **6b1**. These data can be obtained free of charge via http://www.ccdc.cam.ac.uk/conts/retrieving.html, or from the Cambridge Crystallographic Data Centre, 12 Union Road, Cambridge CB2 1EZ, UK; fax: (+44) 1223−336−033; or e−mail: deposit@ccdc.cam.ac.uk.

References

[1] E. Sappa, J. Clust. Sci. 5 (1994) 211. And references therein.

[2] E. Sappa, A. Tiripiccho, P. Braustein, Chem. Rev. 83 (1983) 203. And references therein.

[3] P. Braunstein, L. A. Oro and P. R. Raithby, Metal Clusters in Chemistry, Wiley-VCH Weinheim, Germany, 1999.

[4] P.R. Raithby, M.J. Rosales, Adv. in Inorg. Chem. and Radiochem. 29 (1985) 169. And references therein.

[5] G. Sánchez-Cabrera, F.J. Zuno-Cruz, M.J. Rosales-Hoz, J. Clust. Sci. 25 (2014) 51.

[6] G. Gervasio, E. Sappa, A. Secco, J. Organomet. Chem. 751 (2014) 111.

[7] S. Deabate, R. Giordano, E. Sappa, J. Clust. Sci. 8 (1997) 407.

[8] M. Hernández-Sandoval, G. Sánchez-Cabrera, M.J. Rosales-Hoz, M.A. Leyva, V. Salazar, J.G. Alvarado-Rodríguez, F.J. Zuno-Cruz, Polyhedron 52 (2013) 170.

[9] M.I. Bruce, P.A. Humphrey, H. Miyamae, A.H. White, J. Organomet. Chem. 417 (1991) 431.

[10] C. Jangala, E. Rosenberg, D. Skinner, S. Aime, L. Milone, E. Sappa, Inorg. Chem. 19 (1980) 1571.

[11] M.I. Bruce, N.N. Zaitseva, B.W. Skelton, A.H. White, J. Organomet. Chem. 536 (1997) 93.

[12] G. Gervasio, R. Giordano, D. Marabello, E. Sappa, J. Organomet. Chem. 588 (1999) 83.

[13] I. Torres-Sandoval, S.K. Brayshaw, P.R. Raithby, M.J. Rosales-Hoz, J. Organomet. Chem. 695 (2010) 156.

[14] R. Rosseto, M.D. Vargas, J. Organomet. Chem. 689 (2004) 111.

[15] S.G. Bott, H. Shen, R.A. Senter, M.G. Richmond, Organometallics 22 (2003) 1953.

[16] M. Castiglioni, R. Giordano, E. Sappa, J. Organomet. Chem. 342 (1988) 111.

[17] Z. Otwinowski, W. Minor, Methods in Enzymology, Vol. 276, Macromolecular Crystallography, Part A, New York: Academic Press., 1997, p. 307.

[18] G. M. Sheldrick, Acta Cryst. A 64 (2008) 112.

[19] Sheldrick, G.M, Acta Cryst. C 71 (2015) 3.

[20] Bruker; SAINT (version 8.27B), 2015, BrukerAXS Inc., Madison, Wisconsin, USA.

[21] Bruker; APEX3 (Version 2016.1), 2015, BrukerAXS Inc., Madison, Wisconsin, USA.

[22] Bruker; SADABS (version 2012/1), 2015, BrukerAXS Inc., Madison, Wisconsin, USA.

[23] L. J. Farrugia, J. Appl. Cryst. 32 (1999) 837.

[24] O.V. Dolomanov, L.J. Bourhis, R.J. Gildea, J.A.K. Howard, H. Puschmann, J. Appl. Cryst. 42 (2009) 339.

[25] Sheldrick, G.M, Acta Cryst. A 71 (2015) 3.

[26] A.J. Carty, S.A. MacLaughlin, N.J. Taylor, E. Sappa, Inorg. Chem. 20 (1981) 4437.

[27] L.J. Farrugia, S.E. Rae, Organometallics 11 (1992) 196.

[28] F.J. Zuno-Cruz, A.L. Carrasco, M.J. Rosales-Hoz, Polyhedron 21 (2002) 1105.

[29] M. Hernández-Sandoval, F.J. Zuno-Cruz, M.J. Rosales-Hoz, M.A. Leyva, N. Andrade, V. Salazar, G. Sánchez-Cabrera, J. Organomet. Chem. 696 (2011) 4070.

[30] Cell parameter: Space group P-1. Lengths (Å) and angles (°): a 13.3444(17), b 13.5008(18), c 15.414(2), α 98.766(11), β 92.65(1), γ 106.040(11). Volume 2626.24 Å.

[31] R.T. Morrison, R.N. Boyd, Organic Chemistry; 6a ed. ed., Prentice-Hall Inc. New Jersey, 1992, p. 78, 273, 425.

[32] W.H. Watson, J.-Ch. Wang, M.G. Richmond, J. Chem. Cryst. 33 (2003) 957.

[33] M.I. Bruce, P.J. Low, N.N. Zaitseva, S. Kahlal, J.-F. Halet, B.W. Skelton, A.H. White, J. Chem. Soc., Dalton Trans. (2000) 2939.

[34] H. Li, F.-L. Ting, C.-L. Ho, Y. H. Lo, H.-Y. Lam, N. Zhu, M.-S. Cheung, Z. Lin, W.-Y. Wong, J. Cluster Sci. 26 (2015) 291.

[35] Ch.-K. Wong, G.-L. Lu, Ch.-L. Ho, W.-Y. Wong, Z. Lin, J. Cluster Sci. 23 (2012) 885.

[36] Ch.-K. Wong, G.-L. Lu, C.-L. Ho, W.-Y. Wong, Z. Lin, J. Cluster Sci. 21 (2010) 461.

[37] P. Srinivasan, W. K. Leong, Eur. J. Inorg. Chem. (2006) 464.

[38] E. Delgado, B. Donnadieu, E. Hernandez, M.P. Martin, F. Zamora, Acta Crystallogr., Sect. E: Struct. Rep. Online 58 (2002) m571.

[39] M. Akita, S. Sugimoto, H. Hirakawa, S. Kato, M. Terada, M. Tanaka, and Y. Moro-oka, Organometallics 20 (2001) 1555.

[40] M.I. Bruce, B.W. Skelton, A.H. White, N.N. Zaitseva, J.Organomet.Chem. 650 (2002) 188.

[41] S. Bock, C.F. Mackenzie, B.W. Skelton, L.T. Byrne, G.A. Koutsantonis, P.J. Low, J. Organomet. Chem. 812 (2016) 190.

[42] M.I. Bruce, M. Gaudio, B.W. Skelton, A. Werth, A.H. White, Z. Anorg. Allg. Chem. 634 (2008) 1106.

[43] W.M. Khairul, L. Porres, D. Albesa-Jove, M.S. Senn, M. Jones, D.P. Lydon, J.A.K. Howard, A. Beeby, T.B. Marder, P.J. Low, J. Cluster Sci. 17 (2006) 65.

[44] L.J. Farrugia, CCDC 995547: Experimental Crystal Structure Determination (2014) DOI: 10.5517/cc12dyfv.

[45] L. Xu, S. Li, L. Jiang, G. Zhang, W. Zhang, Z. Gao, RSC Adv. 8 (2018) 4354.

[46] J. Yang, W. Zhang, G. Zhang, Z. Gao, J. Organomet. Chem. 799-800 (2015) 166.

[47] G. Gervasio, D. Marabello, E. Sappa, A. Secco, J. Organomet. Chem. 690 (2005) 1594.

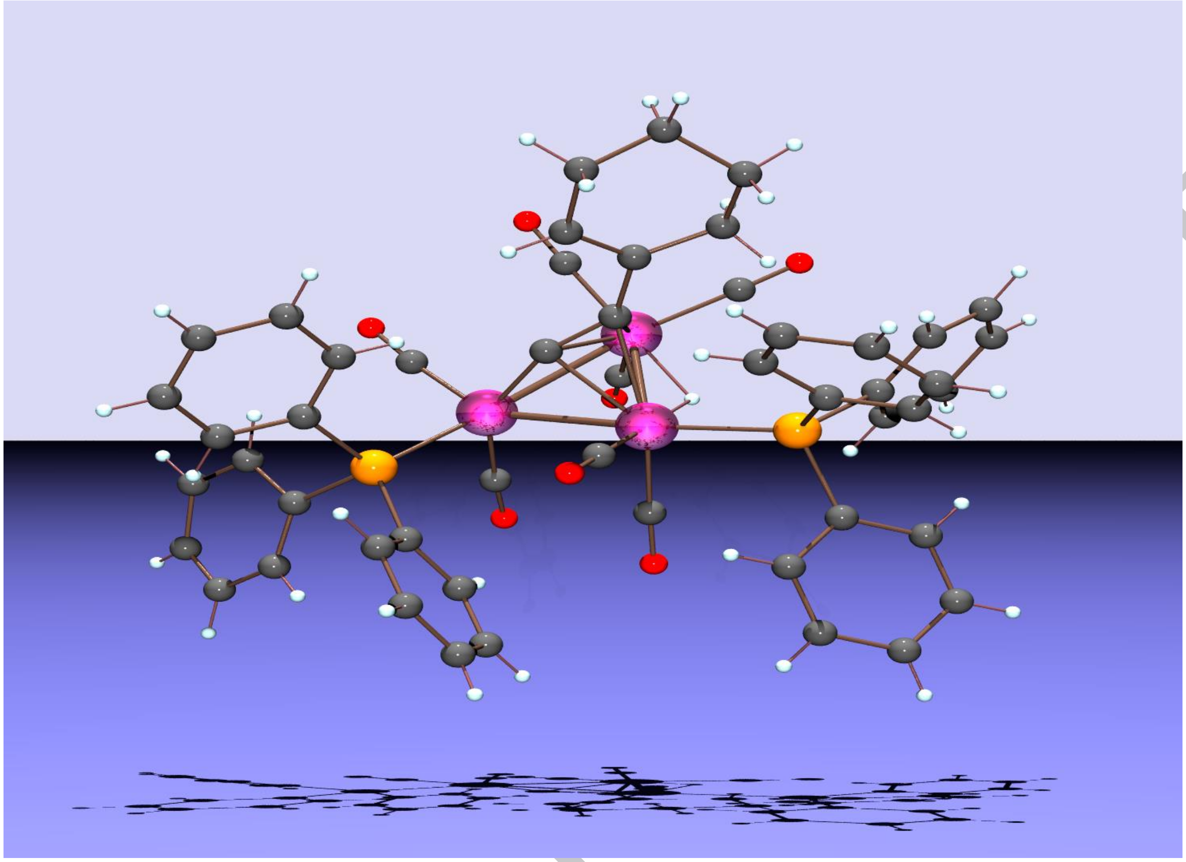

Graphical abstract synopsis

Six series of parallel acetylene and perpendicular acetylide ruthenium trinuclear carbonyl and phosphine clusters have been synthesized. All complexes were fully characterized by IR, NMR, and mass spectrometry. An analysis of the $^{13}C\{^1H\}$ NMR chemical shifts of C_α and C_β was carried out. The molecular structures of the μ_3–η^2–(⊥) perpendicular acetylide cluster **2b**, the monophosphine substituted compounds **4a1**, **4c1** and the disubstituted derivative **6b1** were determined by single crystal X–ray diffraction studies. The stability of μ_3–η^2–(//) parallel acetylene coordination mode in trinuclear ruthenium clusters is increased by the presence of phosphine ligands, which allowed us to characterize the parallel derivatives and determine the molecular structure of monophosphine clusters **3a1** and **3b1** in solid state.